

# Super-Droplet Method for the Numerical Simulation of Clouds and Precipitation: a Particle-Based Microphysics Model Coupled with Non-hydrostatic Model

Shin-ichiro Shima,\* Kanya Kusano, Akio Kawano, Tooru Sugiyama, and Shintaro Kawahara  
*The Earth Simulator Center, Japan Agency for Marine-Earth Science and Technology, Yokohama, Japan*

A novel simulation model of cloud microphysics is developed, which is named Super-Droplet Method (SDM). SDM enables accurate calculation of cloud microphysics with reasonable cost in computation. A simple SDM for warm rain, which incorporates sedimentation, condensation/evaporation, stochastic coalescence, is developed. The methodology to couple SDM and a non-hydrostatic model is also developed. It is confirmed that the result of our Monte Carlo scheme for the coalescence of super-droplets agrees fairly well with the solution of stochastic coalescence equation. A preliminary simulation of a shallow maritime cumulus formation initiated by a warm bubble is presented to demonstrate the practicality of SDM. Further discussions are devoted for the extension and the computational efficiency of SDM to incorporate various properties of clouds, such as, several types of ice crystals, several sorts of soluble/insoluble CCNs, their chemical reactions, electrification, and the breakup of droplets. It is suggested that the computational cost of SDM becomes lower than spectral (bin) method when the number of attributes  $d$  becomes larger than some critical value, which may be  $2 \sim 4$ .

## I. INTRODUCTION

Although clouds play a crucial role in atmospheric phenomena, the numerical modeling of cloud is not well established up to the present. The macro-scale processes such as the fluid motion of moist air associated with clouds is called "cloud dynamics" and the micro-scale processes such as condensation/evaporation, stochastic coalescence, and sedimentation of water droplets, are called "cloud microphysics". These two processes mutually affect each other, and thus we can say that cloud formation and precipitation development are typical multiscale-multiphysics phenomena. Cloud dynamics model to describe the fluid motion in the atmosphere has been well developed (Jacobson 2005). However, it is still difficult to perform an accurate simulation of cloud microphysics though several simulation methods, such as bulk parameterization method (Kessler 1969; Ziegler 1985; Murakami 1990; Ferrier 1994; Meyers et al. 1997), spectral (bin) method (Berry 1967; Soong 1974; Bott 1998, 2000), and the exact Monte Carlo method (Gillespie 1975; Seeßelberg et al. 1996), have been proposed. Numerical methods to accurately simulate both processes and their interactions are required to understand and predict cloud-related phenomena.

We have developed a novel, particle-based simulation model of cloud microphysics, named Super-Droplet Method (SDM), which enables accurate numerical simulation of cloud microphysics with reasonable cost in computation. Though several extensions and validations are still necessary, we expect that SDM provides us a new approach to the cloud-related open problems, such as the cloud and aerosol interactions, the cloud-related radiative processes, and the mechanism of thunderstorms and

lightning.

SDM can be regarded as a sort of Direct Simulation Monte Carlo (DSMC) method, which was initially proposed to simulate the Boltzmann equation for predicting rarefied gas flows (Bird 1994). Particularly, SDM has similarity to the Extended version of the No-Time-Counter (ENTC) method, which was developed by Schmidt and Rutland (2000) for the simulation of spray flows. Though the basic idea of using a computational particle with varying multiplicity is common in both SDM and ENTC, there is a difference in the procedure of the Monte Carlo scheme.

The main purpose of the present paper is to develop a simple SDM for warm rain, which incorporates sedimentation, condensation/evaporation, and stochastic coalescence, and discuss the theoretical foundations of SDM. The methodology to couple SDM and the non-hydrostatic model is also developed. Further discussions on the extensions and the computational efficiency of SDM are also carried out, even though briefly.

The organization of the present paper is as the following. In Sec. II we introduce *the principle model*, which is a very primitive microphysics-macrodynamics coupled cloud model and a good starting point for our discussions. In Sec. III we review the traditional methods, i.e., the exact Monte Carlo method, bulk parameterization method, and spectral (bin) method and see how they are derived from the principle model and what are the problems they involve. In Sec. IV, we develop a simple SDM for warm rain, which can be regarded as a coarse-grained model of the principle model, and discuss the theoretical foundation and characteristics of SDM. Numerical simulation scheme is also proposed for each process. Especially, a novel Monte Carlo scheme for the stochastic coalescence process is developed and validated. In Sec. V a very preliminary result of a shallow maritime cumulus formation initiated by a warm bubble is presented to demonstrate the practicality of SDM. In Sec. VI we briefly discuss the possibility to extend SDM to incorporate various proper-

---

\*Electronic address: s.shima@jamstec.go.jp

ties of clouds, such as, several types of ice crystals, several sorts of soluble/insoluble CCNs, their chemical reactions, electrification, and the breakup of droplets. The estimation of the computational cost of SDM suggests that SDM will be computationally more efficient compared to spectral (bin) method when the number of attributes  $d$  becomes larger than some critical value, which may be  $2 \sim 4$ . Finally, a summary and concluding remarks are presented in Sec. VII.

## II. THE PRINCIPLE MODEL

This section is devoted for the introduction of *the principle model*. The principle model is a very primitive microphysics-macrodynamics coupled cloud model. The characteristic point of this model is the very precise descriptions of cloud microphysics processes, which is realized by following all the water droplets in the atmosphere. Though being not so useful because of the high cost in computation, this model gives us a clear overview of the relationship between each methods to be introduced later, i.e., the exact Monte Carlo method, bulk parameterization method, spectral (bin) method, and super-droplet method.

### A. cloud microphysics for the principle model

#### 1. definition of real-droplets

Warm clouds and rain consist of large number of water droplets with broad range of radius from micrometers to several millimeters. Several sorts of aerosol particles are also floating in the atmosphere, which can be a seed of a cloud droplet. These particles are called Cloud Condensation Nuclei (CCN). We regard each of these particles including both water droplets and CCNs as a real-droplet.

Let  $N_r(t)$  be the number of real-droplets floating in the atmosphere at time  $t$ . Each real-droplet is located at position  $\mathbf{x}_i(t)$ ,  $i = 1, 2, \dots, N_r(t)$ , with velocity  $\mathbf{v}_i(t)$  and radius  $R_i(t)$ . Soluble CCN is dissolved in each real-droplets. Here, we consider only one soluble substance as the CCN and  $M_i$  denotes the mass of solute dissolved in the real-droplet  $i$ . We refer to these state variables, the velocity  $\mathbf{v}_i(t)$ , the radius  $R_i(t)$ , and the mass of solute  $M_i(t)$ , as the attributes of real-droplets denoted by  $\mathbf{a}_i(t)$ . Note that we do not regard the position  $\mathbf{x}_i(t)$  as an attribute for convenience. Assuming that the droplet velocity immediately reaches their terminal velocity,  $\mathbf{v}_i(t)$  is determined by their radius  $R_i(t)$ . As a result, the number of independent attributes of our real-droplet is two, the radius  $R_i(t)$  and the mass of solute  $M_i(t)$ . In the following, we give the time evolution law of real-droplets.

#### 2. motion of real-droplets

In general, the motion equation of a real-droplet is determined by the drag force from the ambient air and the gravitational force:

$$m_i \frac{d\mathbf{v}_i}{dt} = m_i \mathbf{g} + \mathbf{F}_D(\mathbf{v}_i, \mathbf{U}(\mathbf{x}_i), R_i), \quad \frac{d\mathbf{x}_i}{dt} = \mathbf{v}_i, \quad (1)$$

where  $m_i := (4\pi/3)R_i^3\rho_{\text{liq}}$  is the mass of the droplet  $i$  with  $\rho_{\text{liq}} = 1.0 \text{ g cm}^{-3}$ ,  $\mathbf{g}$  is the gravitational constant,  $\mathbf{F}_D$  is the atmospheric drag, and  $\mathbf{U}(\mathbf{x}_i)$  is the wind velocity at the droplet position  $\mathbf{x}_i(t)$ . Assuming that all the droplets reach their terminal velocity immediately enough,  $\mathbf{v}_i(t)$  is evaluated as  $\mathbf{v}_i(t) = \mathbf{U}(\mathbf{x}_i) - \hat{\mathbf{z}}v_\infty(R_i)$ , which is the steady solution of (1). We give  $v_\infty(R_i)$  according to the semi-empirical formulas developed by Beard (1976). Consequently,  $\mathbf{v}_i(t)$  is no longer an independent attribute of real-droplet in our model.

#### 3. condensation/evaporation of real-droplets

We consider the mass change of real-droplets through the condensation/evaporation process according to Köheler's theory, which takes into account the solution and curvature effects on the droplet's equilibrium vapor pressure (Köheler 1936; Rogers and Yau 1989). The growth equation of the radius  $R_i$  is derived as the following.

$$R_i \frac{dR_i}{dt} = \frac{(S-1) - \frac{a}{R_i} + \frac{b}{R_i^3}}{F_k + F_d}, \quad (2)$$

$$F_k = \left( \frac{L}{R_v T} - 1 \right) \frac{L \rho_{\text{liq}}}{K T}, \quad F_d = \frac{\rho_{\text{liq}} R_v T}{D e_s(T)}.$$

Here,  $S$  is the ambient saturation ratio;  $F_k$  represents the thermodynamic term associated with heat conduction;  $F_d$  is the term associated with vapor diffusion; the term  $a/R_i$  represents the curvature effect which expresses the increase in saturation ratio over a droplet as compared to a plane surface; the term  $b/R_i^3$  shows the reduction in vapor pressure due to the presence of a dissolved substance and  $b$  depends on the mass of solute  $M_i$  dissolved in the droplet. Numerically,  $a \simeq 3.3 \times 10^{-5}/T$  (cm) and  $b \simeq 4.3iM_i/m_s$  (cm<sup>3</sup>), where  $T$  (K) is the temperature,  $i \simeq 2$  is the degree of ionic dissociation,  $m_s$  is the molecular weight of the solute.  $R_v$  is the individual gas constant for water vapor,  $K$  is the coefficient of thermal conductivity of air,  $D$  is the molecular diffusion coefficient,  $L$  is the latent heat of vaporization, and  $e_s(T)$  is the saturation vapor pressure.

#### 4. stochastic coalescence of real-droplets

Two real-droplets may collide and coalesce into one big real-droplet and this process is responsible for precipitation development. It is worth noting here that the

coalescence process is of our particular concern in this paper because SDM is expected to overcome the difficulty in the numerical simulation of coalescence process.

Our primary postulate, which is commonly used in many previous studies, is that the coalescence process can be described in a probabilistic way. Consider a region with volume  $\Delta V$  which is small enough compared to the space-scale of the atmospheric fluid. Then, we assume that the real-droplets inside this region are well-mixed and coalesce with each other with some probability during a sufficiently short time interval  $(t, t + \Delta t)$ , i.e., there exists such  $C(R_j, R_k)$  that satisfies

$$\begin{aligned} P_{jk} &= C(R_j, R_k) |\mathbf{v}_j - \mathbf{v}_k| \frac{\Delta t}{\Delta V} \\ &= K(R_j, R_k) \frac{\Delta t}{\Delta V} \\ &= \text{probability that real-droplet } j \text{ and } k \\ &\quad \text{inside the small region } \Delta V \text{ will coalesce} \\ &\quad \text{in the short time interval } (t, t + \Delta t). \end{aligned} \quad (3)$$

Here,  $C(R_j, R_k)$  can be regarded as the effective collision cross-section of the real-droplets  $j$  and  $k$  and may be evaluated as

$$C(R_j, R_k) = E(R_j, R_k) \pi (R_j + R_k)^2, \quad (4)$$

where  $E(R_j, R_k)$  is the collection efficiency, which takes into account the effect that a smaller droplet would be swept aside by the stream flow around the larger droplet or bounce on the surface (Davis 1972; Hall 1980; Jonas 1972; Rogers and Yau 1989).  $K(R_j, R_k)$  is defined by  $K(R_j, R_k) := C(R_j, R_k) |\mathbf{v}_j - \mathbf{v}_k|$  and it is called the coalescence kernel, which will later appear in the stochastic coalescence equation.

The cloud microphysical process of the principle model has been defined. We will turn to determine the cloud dynamics process of the principle model.

## B. cloud dynamics of the principle model

We may apply non-hydrostatic model to describe the cloud dynamics process of the principle model. There are several versions of non-hydrostatic model, but the basic equations used in this paper is as the following.

$$\rho \frac{D\mathbf{U}}{Dt} = -\nabla P - (\rho + \rho_w) \mathbf{g} + \lambda \nabla^2 \mathbf{U}, \quad (5)$$

$$P = \rho R_d T, \quad (6)$$

$$\frac{D\theta}{Dt} = -\frac{L}{c_p \Pi} S_v + \kappa \nabla^2 \theta, \quad (7)$$

$$\frac{D\rho}{Dt} = -\rho \nabla \cdot \mathbf{U}, \quad (8)$$

$$\frac{Dq_v}{Dt} = S_v + \kappa \nabla^2 q_v. \quad (9)$$

Here,  $D/Dt := \partial/\partial t + \mathbf{U} \cdot \nabla$  is the material derivative;  $\rho = \rho_d + \rho_v$  is the density of moist air, which is represented by the sum of dry air density  $\rho_d$  and vapor density  $\rho_v$ ;  $q_v = \rho_v/\rho$  is the mixing ratio of vapor;  $\mathbf{U}$  is the wind velocity;  $T$  is the temperature;  $\theta$  is the potential temperature;  $\Pi = (P/P_0)^{(R_d/c_p)}$  is the Exner function with reference pressure  $P_0$ ;  $\rho_w$  is the density of liquid water;  $S_v$  is the source term of water vapor associated with condensation/evaporation process;  $\mathbf{g}$  is the gravitational constant;  $\lambda$  and  $\kappa$  are the transport coefficient;  $R_d$  is the gas constant for dry air;  $c_p$  is the specific heat of dry air at constant pressure;  $L$  is the latent heat of vaporization. Equations (5)-(9) represent equation of motion, equation of state, thermodynamic equation, mass continuity, and water continuity, respectively. Note here that it is assumed that  $q_v \ll 1$  to derive these equations.

There are three coupling terms from the microphysics:  $\rho_w$  represents the momentum coupling;  $LS_v/c_p \Pi$  is the release of latent heat through the condensation/evaporation process;  $S_v$  is the source term of vapor through the condensation/evaporation process. These source terms are evaluated by the microphysics variables,

$$\rho_w(\mathbf{x}, t) := \sum_{i=1}^{N_r} m_i(t) \delta^3(\mathbf{x} - \mathbf{x}_i(t)), \quad (10)$$

$$S_v(\mathbf{x}, t) := \frac{-1}{\rho(\mathbf{x}, t)} \frac{\partial \rho_w}{\partial t}(\mathbf{x}, t), \quad (11)$$

where  $m_i$  is the mass of real-droplet  $i$ .

The principle model has defined completely now and we can see that the description of the cloud microphysics is very precise. In the next section, we review the traditional methods from the point of view how they are related to the principle model.

## III. TRADITIONAL METHODS

In this section, we review the traditional methods and see how they are derived from the principle model and what are the problems involved.

### A. The exact Monte Carlo method

The exact Monte Carlo method was developed by Gillespie (1975) and improved by Seefelberg et al. (1996). This method simulates the principle model very directly. Their procedure repeatedly draws a random waiting time for which the next one pair of real-droplets will coalesce. Consequently, it is very rigorous, but not so useful to simulate a cloud formation process in a sufficiently large region because of the very high cost in computation.

## B. bulk parameterization method

Bulk parameterization method is most commonly used to deal with cloud microphysics. This method empirically evaluates the source terms from microphysics, such as  $\rho_w$  and  $S_v$ , as a function of the field variables in the cloud dynamics model (Kessler 1969; Ziegler 1985; Murakami 1990; Ferrier 1994; Meyers et al. 1997). Then, the governing equations become a closed form in cloud dynamics variables and we need not cope directly with cloud micro-physics. Consequently, the number of degrees of freedom is reduced so much that the computational demand is extremely relaxed. However, the accuracy seems to be not always enough. This is very likely because bulk parameterization is justified under the assumption that there exists a closed-form equation in cloud dynamics, though this is not guaranteed.

## C. spectral (bin) method

Another approach to cloud microphysics is spectral (bin) method (Berry 1967; Soong 1974; Bott 1998, 2000). Spectral (bin) method is characterized by solving the time evolution equation of the number density distribution of real-droplets.

Let  $X_i = (4\pi/3)R_i^3$  be the volume of the real-droplet  $i$ , and  $n(X, M, \mathbf{x}, t)$  be the number density distribution of real-droplets, i.e.,  $n(X, M, \mathbf{x}, t)\Delta X \Delta M \Delta V$  denotes the number of real-droplets with their volume in the range of  $(X, X + \Delta X)$ , mass of solute in the range of  $(M, M + \Delta M)$ , inside the space region  $\Delta V$  around  $\mathbf{x}$ , at time  $t$ . Then, the time evolution equation for  $n(X, M, \mathbf{x}, t)$  which corresponds to the principle model can be derived as the following.

$$\begin{aligned} & \frac{\partial n}{\partial t} + \nabla_{\mathbf{x}} \cdot \{\mathbf{v}_t(X, \mathbf{x})n\} + \frac{\partial}{\partial X} \{f_g(X, M, \mathbf{x})n\} \\ &= \frac{1}{4} \int_0^M dM' \int_0^X dX' n(X', M')n(X'', M'')K(X', X'') \\ & \quad - n(X, M) \int_0^\infty dM' \int_0^\infty dX' n(X', M')K(X, X'), \end{aligned} \quad (12)$$

where  $\mathbf{v}_t(X, \mathbf{x}) := \mathbf{U}(\mathbf{x}) - \hat{z}v_\infty(R)$  is the terminal velocity of a droplet,  $f_g(X, M, \mathbf{x}) := 4\pi R \times$  (r.h.s of (2)) satisfies  $dX/dt = f_g$ ,  $K$  is the coalescence kernel defined in (3),  $X'' := X - X'$ , and  $M'' := M - M'$ . The l.h.s of (12) corresponds to the advection of real-droplets in real-space and attribute-space, and the r.h.s corresponds to the expected dynamics of the stochastic coalescence process.

On the ideal case when there is only the stochastic coalescence process and neither sedimentation nor condensation/evaporation process exists, and further, only the droplet volume  $X$  is regarded as the attribute, then

(12) reduces to

$$\begin{aligned} \frac{\partial n(X, t)}{\partial t} &= \frac{1}{2} \int_0^X dX' n(X')n(X'')K(X', X'') \\ & \quad - n(X) \int_0^\infty dX' n(X')K(X, X'). \end{aligned} \quad (13)$$

This is the simplest case of spectral (bin) method and (13) is the equation which is sometimes called the stochastic coalescence equation (SCE), but in this paper, SCE is used as a general term refers to the governing equation of spectral (bin) method.

These equations are derived from the probability law (3) under the assumption that the number density has no correlation (Gillespie 1972). This assumption seems to be correct (Seeßelberg et al. 1996), thus the solution of SCE can be very accurate. However, the computational cost to solve SCE is very expensive, especially if we consider many types of microphysics processes and the number of attributes  $d$  becomes large. We will come back to this remark in Sec. VI, but in a word, this is owing to the fact that the governing equation contains a  $d$ -multiple integral.

## IV. SUPER-DROPLET METHOD

In this section, we develop a simple SDM for warm rain, which can be regarded as a coarse-grained model of the principle model, and discuss the theoretical foundation and characteristics of SDM. Numerical simulation scheme is also proposed for each process. Especially, a novel Monte Carlo scheme for the stochastic coalescence process is developed and validated.

### A. cloud microphysics for Super-Droplet Method

#### 1. definition of super-droplets

First of all, let us define what a super-droplet is. Each super-droplet represents a multiple number of real-droplets with the same attributes and position, and the multiplicity is denoted by the positive integer  $\xi_i(t) \in \{1, 2, \dots\}$ , which value can be different in each super-droplet and time-dependent due to the definition of coalescence introduced later. That is to say, each super-droplet has their own position  $\mathbf{x}_i(t)$  and own attributes  $\mathbf{a}_i(t)$ , which characterize the  $\xi_i(t)$  number of same real-droplets represented by the super-droplet  $i$ . Here, the attribute  $\mathbf{a}_i(t)$  consists of the radius  $R_i(t)$  and the solute mass  $M_i(t)$  for this simplest case. Note here that no two real-droplets have exactly the same position and attributes. In this sense, super-droplet is a kind of coarse-grained view of real-droplets both in real-space and attribute-space. Let  $N_s(t)$  be the number of super-droplets floating in the atmosphere at time  $t$ . Then, these super-droplets represent  $N_r(t) = \sum_{i=1}^{N_s(t)} \xi_i(t)$  number of

real-droplets in total. In the following, we give the time evolution law of the super-droplets.

## 2. motions of super-droplets

Except the coalescence process, each super-droplet behaves just like a real-droplet. Thus, a super-droplet moves according to the motion equation (5) and  $\mathbf{v}_i(t)$  is evaluated by the terminal velocity.

It is easy to simulate this process numerically. Define the time step  $\Delta t_m$  and evaluate the terminal velocity  $\mathbf{v}_i(t)$  and the position  $\mathbf{x}_i(t + \Delta t_m) = \mathbf{x}_i(t) + \Delta t_m \mathbf{v}_i(t)$  at each time step.

## 3. condensation/evaporation of super-droplets

Condensation/evaporation process of super-droplets is also governed by the growth equation (2).

We may adopt implicit Euler discretization scheme for the numerical simulation of (2), yielding

$$\frac{R_{i,n+1}^2 - R_{i,n}^2}{2\Delta t_g} = \frac{(S-1) - \frac{a}{R_{i,n+1}} + \frac{b}{R_{i,n+1}^3}}{F_k + F_d},$$

where  $R_{i,n} \simeq R_i(t = n\Delta t_g)$ . It may be not possible to determine analytically the next step value  $R_{i,n+1}$  from the previous value  $R_{i,n}$ . However, using Newton-Raphson scheme,  $R_{i,n+1}$  can be evaluated numerically.

## 4. stochastic coalescence of super-droplets

Stochastic coalescence process for the super-droplets must be formulated carefully so that the super-droplets well-approximate the behavior of real-droplets. The formulation procedure is in two steps: 1) define how a pair of super-droplets coalesce; 2) determine the probability that the super-droplet coalescence occurs.

Consider the case when a pair of super-droplets  $(j, k)$  will coalesce. These super-droplets represent  $\xi_j$  number of real-droplets  $(\mathbf{a}_j, \mathbf{x}_j)$  and  $\xi_k$  number of real-droplets  $(\mathbf{a}_k, \mathbf{x}_k)$ . Let us define that exactly  $\min(\xi_j, \xi_k)$  pairs of real-droplets will contribute to the coalescence of the super-droplet pair  $(j, k)$ . Figure. 1 is a schematic view of the coalescence of super-droplets. In this example,  $\xi_j = 3$  and  $\xi_k = 2$ . We can see that  $\min(\xi_j, \xi_k) = 2$  pairs of real-droplets undergo coalescence, which results in the decrease of multiplicity  $\xi_j : 3 \rightarrow 1$  and the increase of the size of the super-droplet  $k$ .

Below is the complete definition of how a pair of super-droplets  $(j, k)$  change their state after the coalescence:

1. if  $\xi_j \neq \xi_k$ , we can choose  $\xi_j > \xi_k$  without losing

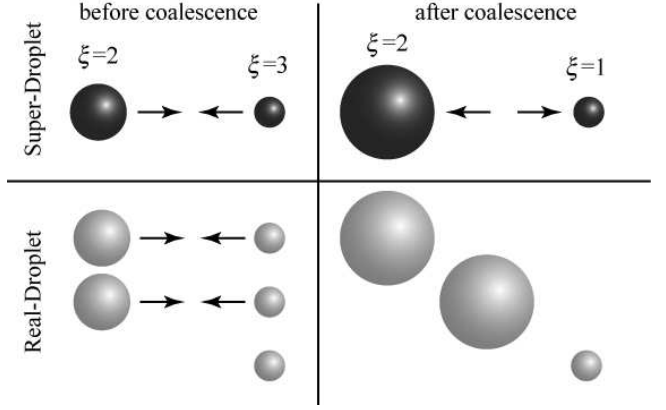


FIG. 1: Schematic view of the coalescence of super-droplets. Two super-droplets with multiplicity 2 and 3 undergo coalescence (upper left). This represents the coalescence of 2 real-droplet pairs (lower left and right). As a result the super-droplet with multiplicity 2 becomes larger and the multiplicity of the other super-droplet decreases  $3 \rightarrow 1$  (upper right).

generality, and

$$\xi'_j = \xi_j - \xi_k, \quad \xi'_k = \xi_k, \quad (14)$$

$$R'_j = R_j, \quad R'_k = (R_j^3 + R_k^3)^{1/3}, \quad (15)$$

$$M'_j = M_j, \quad M'_k = (M_j + M_k), \quad (16)$$

$$\mathbf{x}'_j = \mathbf{x}_j, \quad \mathbf{x}'_k = \mathbf{x}_k, \quad (17)$$

where the dashed values represent the updated value after the coalescence.

2. if  $\xi_j = \xi_k$ ,

$$\xi'_j = [\xi_j/2], \quad \xi'_k = \xi_j - [\xi_j/2], \quad (18)$$

$$R'_j = R'_k = (R_j^3 + R_k^3)^{1/3}, \quad (19)$$

$$M'_j = M'_k = (M_j + M_k), \quad (20)$$

$$\mathbf{x}'_j = \mathbf{x}_j, \quad \mathbf{x}'_k = \mathbf{x}_k, \quad (21)$$

where Gauss' symbol  $[x]$  is the greatest integer that is less than or equal to  $x$ .

Note here that in the case  $\xi_j = \xi_k$ , no real-droplets will be left after the coalescence because all  $\xi_j$  number of real-droplets contribute to the coalescence. Thus, we divide the resulting  $\xi_j$  number of real-droplets into two super-droplets.

This definition of super-droplet coalescence possess has a favorable property that the number of super-droplets is unchanged in most cases though the number of real-droplets always decreases. The number of super-droplets is decreased through the coalescence only when  $\xi_j = \xi_k = 1$ , i.e., both super-droplets are real-droplets. This results in  $\xi'_j = 0$  and  $\xi'_k = 1$ , and we remove the super-droplet  $j$  out of the system. Because the number of super-droplets corresponds to the accuracy of SDM, the number conservation of super-droplets suggests the flexible response of SDM to the drastic change of the number of real-droplets.

Having defined how a pair of super-droplets coalesces, we turn to determine the probability that the coalescence occurs. If we require the consistency of the expectation value, the probability is determined as the following.

$$\begin{aligned} P_{jk}^{(s)} &= \max(\xi_j, \xi_k) P_{jk} \\ &= \text{probability that super-droplet } j \text{ and } k \\ &\quad \text{inside the small region } \Delta V \text{ will coalesce} \\ &\quad \text{in the short time interval } (t, t + \Delta t_c). \end{aligned} \quad (22)$$

Indeed, we can confirm that the expectation value is exactly the same to that of the principle model (real-droplet view). The super-droplet  $j$  represents  $\xi_j$  number of real-droplets with attribute  $\mathbf{a}_j$  and super-droplet  $k$  represents  $\xi_k$  number of real-droplets with attribute  $\mathbf{a}_k$ . From the real-droplet view, there are  $\xi_j \xi_k$  number of real-droplet pairs which have the possibility to coalesce with the probability  $P_{jk}$ , i.e., the number of real-droplet pairs which will coalescence follows the binomial distribution with  $\xi_j \xi_k$  trials and success probability  $P_{jk}$ . Thus, from the real-droplet view, the expectation value of the number of coalesced pairs is  $\xi_j \xi_k P_{jk}$ . From the super-droplet view, a coalescence of super-droplets  $j$  and  $k$  represents the coalescence of  $\min(\xi_j, \xi_k)$  pairs of real-droplets with attribute  $\mathbf{a}_j$  and  $\mathbf{a}_k$ . Thus, the coalescence of super-droplets  $j$  and  $k$  is expected to represent  $\min(\xi_j, \xi_k) P_{jk}^{(s)} = \min(\xi_j, \xi_k) \max(\xi_j, \xi_k) P_{jk} = \xi_j \xi_k P_{jk}$  number of coalescence of real-droplet pairs, which is equal to the value of the real-droplet view. It is worth noticing here that the variance of super-droplet view becomes larger than that of real-droplet view. From real-droplet view, the variance of the number of coalesced pairs is  $\xi_j \xi_k P_{jk} (1 - P_{jk}) \simeq \xi_j \xi_k P_{jk} =: V_r$  (Poisson distribution limit). From super-droplet view, the variance is  $\{\min(\xi_j, \xi_k)\}^2 P_{jk}^{(s)} - \{\xi_j \xi_k P_{jk}\}^2 \simeq \min(\xi_j, \xi_k) V_r$ , which is  $\min(\xi_j, \xi_k)$  times larger than that of the real-droplet view.

We have defined the cloud microphysics of super-droplets. If all the multiplicity  $\xi_i = 1$  then our model is equivalent to the principle model. Thus, we can change the accuracy of our model by changing the initial distribution of multiplicity  $\{\xi_i(t=0)\}$ , or equivalently, the initial number of super-droplets  $N_s(t=0)$ . If the convergence to the principle model is rapid, we can say that the use of SDM is beneficial.

The definition of the coalescence process of super-droplets is rather theoretical and we have to do numerical simulation on this model somehow. In the next section, we develop a Monte Carlo scheme for the stochastic coalescence, which can simulate the coalescence process of super-droplets efficiently.

## 5. Monte Carlo Scheme for super-droplet coalescence

Let us introduce a grid which covers the real-space. We can choose any kind of grids, which may be not uniform, but the volume of each cell must be small enough

compared to the space-scale of the atmospheric fluid so that the coalescence occurs according to the probability (22) in each cell. Let us make a list of super-droplets in a certain cell at time  $t$ :  $I := \{i_1, i_2, \dots, i_{n_s}\}$ , where  $n_s$  is the total number of super-droplets in the cell. Then, by definition, each pair of super-droplets  $(j, k) \in I^2$ ,  $j \neq k$ , coalesces with the probability  $P_{jk}^{(s)}$  within the short time interval  $(t, t + \Delta t_c)$ . Note that  $P_{jk}^{(s)} \ll 1$  because  $\Delta t_c$  is small. We have to examine all the possible pairs  $(j, k) \in I^2$ ,  $j \neq k$ , to know the random realization at the time  $t + \Delta t_c$ . However, this yields computational cost  $O(n_s^2)$  and this is not efficient. Instead, we propose a novel Monte Carlo scheme which leads us to  $O(n_s)$  cost in computation.

Let  $L := \{(j_1, k_1), (j_2, k_2), \dots, (j_{[n_s/2]}, k_{[n_s/2]})\}$  be a list of randomly generated, non-overlapping,  $[n_s/2]$  number of pairs. Non-overlapping means that no super-droplet belongs to more than one pair. This list can be made by generating a random permutation of  $I$  and make pairs from the front, which cost  $O(n_s)$  in computation (see the appendix). By examining only these  $[n_s/2]$  pairs instead of the whole possible  $n_s(n_s - 1)/2$  pairs, the cost will be  $O(n_s)$ . In compensation for this simplification, all the coalescence probability is divided by the decreasing ratio of pair number, and the corrected, scaled up probability for the  $\alpha$ th pair is obtained as

$$p_\alpha := P_{j_\alpha k_\alpha}^{(s)} \frac{n_s(n_s - 1)}{2} \Big/ \left[ \frac{n_s}{2} \right]. \quad (23)$$

This may be justified if the following relation holds good,

$$\begin{aligned} \sum_{\alpha=1}^{[n_s/2]} \min(\xi_{j_\alpha}, \xi_{k_\alpha}) p_\alpha &\simeq \frac{1}{2} \sum_{j,k} \sum_{j \neq k} \min(\xi_j, \xi_k) P_{jk}^{(s)} \\ &= \frac{1}{2} \sum_{j,k} \sum_{j \neq k} \xi_j \xi_k P_{jk}, \end{aligned}$$

which represent the consistency of the expectation number of coalesced real-droplet pairs in this cell.

Based on the above idea, below is the complete procedure of our Monte Carlo scheme to obtain one of the stochastic realizations in a certain cell at time  $t + \Delta t_c$  from the state of super-droplets at time  $t$ .

1. Make the super-droplet list at time  $t$  in this certain cell:  $I = \{i_1, i_2, \dots, i_{n_s}\}$ .
2. Make the  $[n_s/2]$  number of candidate-pairs  $L = \{(j_1, k_1), (j_2, k_2), \dots, (j_{[n_s/2]}, k_{[n_s/2]})\}$  from the random permutation of  $I$ .
3. For each pair of super-droplets  $(j_\alpha, k_\alpha) \in L$ , generate a uniform random number  $\phi_\alpha \in (0, 1)$ . Then, evaluate

$$\gamma_\alpha := \begin{cases} [p_\alpha] + 1 & \text{if } \phi_\alpha < p_\alpha - [p_\alpha] \\ [p_\alpha] & \text{if } \phi_\alpha \geq p_\alpha - [p_\alpha] \end{cases}$$

4. If  $\gamma_\alpha = 0$ , the  $\alpha$ th pair  $(j_\alpha, k_\alpha)$  is updated to  $t + \Delta t_c$  without changing their state.
5. If  $\gamma_\alpha \neq 0$ , choose  $\xi_{j_\alpha} \geq \xi_{k_\alpha}$  without losing generality and evaluate  $\tilde{\gamma}_\alpha := \min(\gamma_\alpha, [\xi_{j_\alpha}/\xi_{k_\alpha}])$ .

(a) if  $\xi_{j_\alpha} - \tilde{\gamma}_\alpha \xi_{k_\alpha} > 0$ ,

$$\begin{aligned}\xi'_{j_\alpha} &= \xi_{j_\alpha} - \tilde{\gamma}_\alpha \xi_{k_\alpha}, & \xi'_{k_\alpha} &= \xi_{k_\alpha}, \\ R'_{j_\alpha} &= R_{j_\alpha}, & R'_{k_\alpha} &= (\tilde{\gamma}_\alpha R_{j_\alpha}^3 + R_{k_\alpha}^3)^{1/3}, \\ M'_{j_\alpha} &= M_{j_\alpha}, & M'_{k_\alpha} &= (\tilde{\gamma}_\alpha M_{j_\alpha} + M_{k_\alpha}), \\ \mathbf{x}'_{j_\alpha} &= \mathbf{x}_{j_\alpha}, & \mathbf{x}'_{k_\alpha} &= \mathbf{x}_{k_\alpha},\end{aligned}$$

(b) If  $\xi_{j_\alpha} - \tilde{\gamma}_\alpha \xi_{k_\alpha} = 0$ , i.e.,  $\tilde{\gamma}_\alpha = \xi_{j_\alpha}/\xi_{k_\alpha} = [\xi_{j_\alpha}/\xi_{k_\alpha}] \leq \gamma_\alpha$ ,

$$\begin{aligned}\xi'_{j_\alpha} &= [\xi_{k_\alpha}/2], & \xi'_{k_\alpha} &= \xi_{k_\alpha} - [\xi_{k_\alpha}/2], \\ R'_{j_\alpha} &= R'_{k_\alpha} = (\tilde{\gamma}_\alpha R_{j_\alpha}^3 + R_{k_\alpha}^3)^{1/3}, \\ M'_{j_\alpha} &= M'_{k_\alpha} = (\tilde{\gamma}_\alpha M_{j_\alpha} + M_{k_\alpha}), \\ \mathbf{x}'_{j_\alpha} &= \mathbf{x}_{j_\alpha}, & \mathbf{x}'_{k_\alpha} &= \mathbf{x}_{k_\alpha}.\end{aligned}$$

If  $\xi'_{j_\alpha} = 0$ , the super-droplet  $j_\alpha$  is removed out of the system.

Our Monte Carlo scheme numerically solves the stochastic coalescence process of super-droplets defined in Sec. IV A 4. We used a sort of random sampling of candidate-pairs to achieve the computational cost  $O(n_s)$ . Further extension are implemented in our Monte Carlo scheme to deal with *multiple coalescence*. The integer  $\gamma_\alpha$  represents how many times the pair  $(j_\alpha, k_\alpha)$  will coalesce, and  $\tilde{\gamma}_\alpha$  is the restricted value of  $\gamma_\alpha$  by its maximum value  $[\xi_{j_\alpha}/\xi_{k_\alpha}]$ . Primarily,  $p_\alpha$  must be smaller than 1 because  $p_\alpha$  represents a probability, thus  $\gamma_\alpha$  should be either 0 or 1. However, if we take  $\Delta t_c$  too much larger,  $p_\alpha$  may become larger than 1. Though the situation  $\gamma_\alpha > 1$  is not consistent with the fundamental premise of our theory, we formulate our Monte Carlo scheme to cope with this situation so that SDM robustly well-approximate the principle model irrespective of the choice of  $\Delta t_c$ .

Alternatively be said that the most rigorous selection criteria of the simulation time step for coalescence process  $\Delta t_c$  is that  $p_\alpha \ll 1$  holds good for all  $\alpha$ . Let us estimate  $\Delta t_c$  very roughly. The typical number density and radius of small cloud droplets may be  $10^9 \text{ m}^{-3}$  and  $R = 10 \mu\text{m}$ . The typical terminal velocity of a rain droplet may be  $1 \text{ m s}^{-1}$ . Then, we may roughly evaluate  $p_\alpha$  as follows.

$$\begin{aligned}p_\alpha &\simeq n_s P_{j_\alpha k_\alpha}^{(s)} \\ &= \frac{n_s \max(\xi_{j_\alpha}, \xi_{k_\alpha})}{\Delta V} E \pi (R_{j_\alpha} + R_{k_\alpha})^2 |\mathbf{v}_{j_\alpha} - \mathbf{v}_{k_\alpha}| \Delta t_c \\ &\simeq 10^9 \text{ m}^{-3} \cdot 1 \cdot \pi (2 \times 10^{-5} \text{ m})^2 \cdot 1 \text{ m s}^{-1} \cdot \Delta t_c \\ &= 0.4\pi \Delta t_c < 1.\end{aligned}$$

Thus, it is estimated that  $\Delta t_c < 1/0.4\pi \text{ s} \simeq 0.8 \text{ s}$ . It is worth noticing here, that our estimation is independent of the number of super-droplets  $n_s$  and the volume of the coalescence cell  $\Delta V$ .

## 6. validation of our Monte Carlo scheme

In this section, we validate our Monte Carlo scheme for the stochastic coalescence process by confirming that the numerical results agree well with the solution of the SCE (13).

The SCE (13) is the time evolution equation of  $n(X, t)$  in the ideal system in which only the stochastic coalescence process exists. Correspondingly, the super-droplets in this section undergo only the coalescence process according to our Monte Carlo scheme. The super-droplets have velocities, but do not move out of the coalescence cell, nor do they undergo condensation/evaporation. The radius  $R_i$  is the only attribute.

To compare the simulation result, we have to reconstruct the number density distribution  $n(X, t)$  from the data of super-droplets  $\{(\xi_i, R_i)\}$ . There are several ways to do this, but we adopt kernel density estimate method with Gaussian kernel (Terrell and Scott 1992). Some brief discussions on the application of kernel density estimate method to SDM is also developed in Sec. IV B. It is convenient to plot the results by the mass density function over  $\ln R$ , which is defined by  $g(\ln R) d \ln R := \rho_{\text{liq}} X n(X) dX$ . The corresponding estimator function  $\tilde{g}(\ln R)$  becomes,

$$\begin{aligned}\tilde{g}(\ln R) &:= \frac{1}{\Delta V} \sum_{i=1}^{N_s} \xi_i m_i W_\sigma(\ln R - \ln R_i), \\ W_\sigma(Y) &:= \frac{1}{\sqrt{2\pi}\sigma} \exp(-Y^2/2\sigma^2).\end{aligned}$$

Here,  $\Delta V$  is the volume of the coalescence cell and  $\sigma = \sigma_0 N_s^{-1/5}$  with some constant  $\sigma_0$ . Theoretically, the most efficient choice of  $\sigma_0$  is estimated as  $\sigma_0 = (2\sqrt{\pi}\Delta V^2 \int g''^2 d \ln R / M_{\text{tot}} N_r)^{-1/5}$ , where  $M_{\text{tot}}$  is the total mass of liquid water. Because  $g$  is the estimated function itself, we have to estimate also  $\sigma_0$  from the data of super-droplets to find the maximum likelihood estimator function  $\tilde{g}$ , but in this paper we just choose  $\sigma_0$  empirically.

We have to give an explicit form of the coalescence kernel  $K(R_j, R_k)$  in (3) to determine the dynamics. For Golovin's kernel  $K(R_j, R_k) = b(X_j + X_k)$ , we have the analytic solution of SCE (13) (Golovin 1963) though this choice of coalescence kernel is not realistic. The result of our comparison simulation for Golovin's kernel is shown in Fig. 2a. We set  $b = 1.5 \times 10^3 \text{ s}^{-1}$ . We need only one big coalescence cell, the volume of which is chosen to be  $\Delta V = 10^6 \text{ m}^3$ . The time step is fixed as  $\Delta t_c = 1.0 \text{ s}$ . The initial number density of real-droplets is set to be  $n_0 = 2^{23} \text{ m}^{-3}$ . The initial size distribution of the real-droplets follows an exponential distribution of the droplet volume  $X_i$  which is determined by the probability density  $p(X_i) = (1/X_0) \exp(-X_i/X_0)$ ,  $X_0 = (4\pi/3)R_0^3$ ,  $R_0 = 30.531 \times 10^{-6} \text{ m}$ . This setting results in the total amount of liquid water  $1.0 \text{ g m}^{-3}$ . The initial number of super-droplet  $N_s$  is changed as the simulation parameter.

The initial multiplicity  $\xi_i$  is determined by the equality  $\xi_i = n_0 \Delta V / N_s$ .  $\sigma_0$  is fixed as  $\sigma_0 = 0.62$ .

Figures 2b and 2c show the results of the case of so-called hydrodynamic kernel, which is a much realistic coalescence kernel. Hydrodynamic kernel is defined by (3) and (4). The same coalescence efficiency  $E(R_j, R_k)$  is adopted as described in Seefelberg et al. (1996) and Bott (1998). For small droplets the dataset of Davis (1972) and Jonas (1972) is used, and for large droplets the dataset of Hall (1980) is used. Because the analytic solution is not available for hydrodynamic kernel, we generated the reference solution numerically using Exponential Flux Method (EFM) developed by Bott (1998, 2000). A logarithmically equidistant radius grid is used in EFM. We adopted 1000 bins ranging from  $0.62 \mu\text{m}$  to  $6.34 \text{ cm}$ . The time step was set to  $0.1 \text{ s}$ . These parameter settings provide a sufficiently accurate numerical solution of the SCE (13). In Fig. 2b, simulation settings are same as case (a) except the coalescence kernel. In Fig. 2c we changed the initial size distribution by reducing  $R_0$  to one-third, i.e.,  $R_0 = 10.177 \times 10^{-6} \text{ m}$ , and increased the initial number density of real-droplets as  $n_0 = 3^3 \cdot 2^{23} \text{ m}^{-3}$ . Consequently, the total amount of liquid water  $1.0 \text{ g m}^{-3}$  is unchanged from case (b).  $\Delta t_c = 0.1 \text{ s}$  and  $\sigma_0 = 1.5$  for case (c).

In case (a) and (b), we can see that the result of SDM with  $N_s = 2^{13}$  agrees fairly well with the solution of SCE (13), and much improved when  $N_s = 2^{17}$ . However, case (c) is not so good as the previous two cases. Even  $N_s = 2^{17}$  is not good and we need  $N_s = 2^{21}$  for good agreement. This situation typically reveals the weak point of SDM. The initial size of the droplets are comparatively small and the coalescence hardly occurs. We can see that the thick solid line at  $t = 1200 \text{ s}$  is not so changed from the initial distribution. However, once a few big droplets are created, then the coalescence process is abruptly accelerated. Accordingly, for an accurate prediction, we have to resolve the right tail of the distribution at the time  $t = 1200 \text{ s}$ . However, existence probability of super-droplets is very low for such region and sampling error occurs if the number of super-droplets  $N_s$  is not sufficient. As a result, we need much more super-droplets for case (c) compared to that of (a) and (b). For the practical applications to cloud formation, this fact would not impose severe restrictions on SDM because the condensation/evaporation process dominates the growth of small droplets in such cases like (c).

Anyway, we have confirmed that SDM reproduces the solution of the SCE (13) if the number of super-droplets  $N_s$  is sufficiently large. These results support the validity of our Monte Carlo scheme for the stochastic coalescence.

## B. cloud dynamics for Super-Droplet Method

For the cloud dynamics of SDM, we can also apply the non-hydrostatic model (5)-(9). Note here that we have to evaluate the source terms from microphysics (10)-(11)

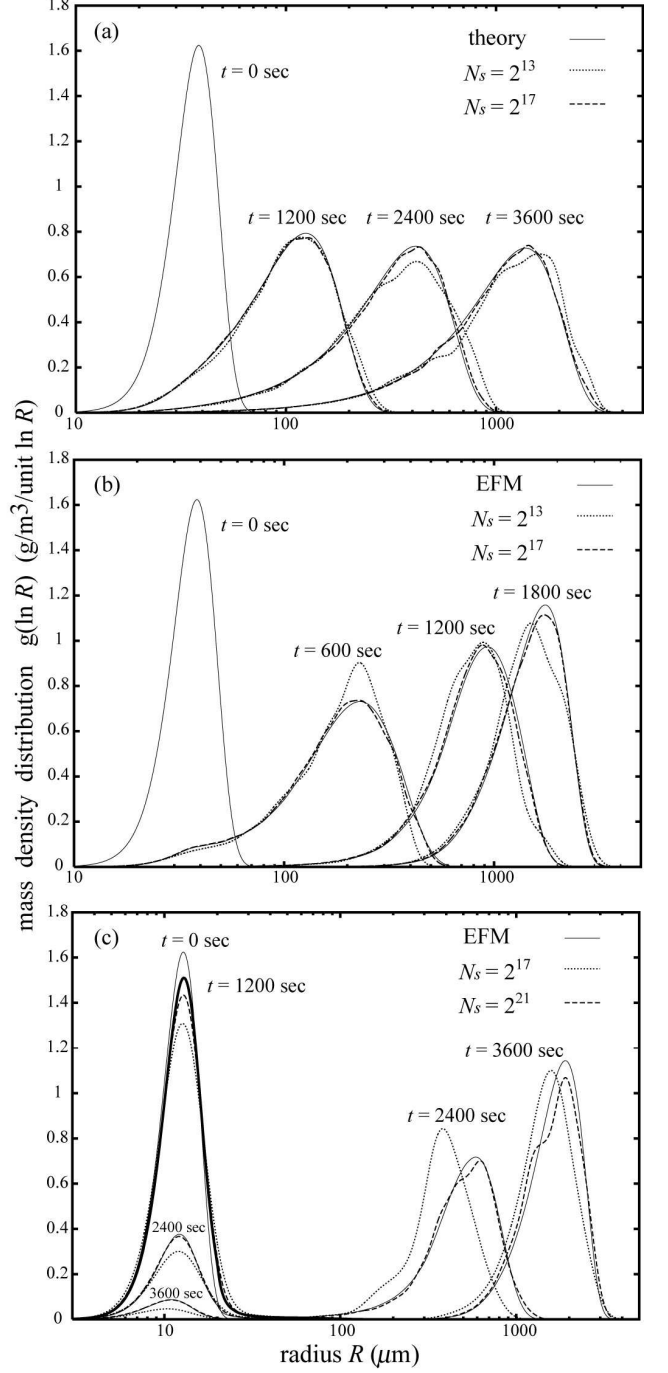


FIG. 2: Time evolution of the mass density distribution  $g(\ln R, t)$ , which is numerically obtained by the Monte Carlo scheme of SDM. (a): The case of Golovin's kernel. The solid line represents the analytic solution of SCE (13). (b) and (c): The case of hydrodynamic kernel. The solid line represents the approximate solution of SCE (13), which is numerically obtained by EFM. In each case, we can see that the result of SDM agrees fairly well with solution of SCE (13) when the number of super-droplets  $N_s$  is sufficiently large.  $\Delta t_c = 1.0 \text{ s}$  for (a) and (b), and  $\Delta t_c = 0.1 \text{ s}$  for (c).

not by real-droplets but by super-droplets:

$$\rho_w(\mathbf{x}, t) = \sum_{i=1}^{N_s} \xi_i m_i(t) \delta^3(\mathbf{x} - \mathbf{x}_i(t)), \quad (24)$$

$$S_v(\mathbf{x}, t) = \frac{-1}{\rho(\mathbf{x}, t)} \frac{\partial \rho_w}{\partial t}(\mathbf{x}, t). \quad (25)$$

For the numerical simulation of (5)-(9), we may adapt 4th-order Runge-Kutta scheme for the time derivative, second-order central difference scheme for the spatial derivatives, with artificial viscosity to stabilize the numerical instability. The source terms (24) and (25) must be evaluated on the numerical grid point of fluid simulation  $\mathbf{x}_j^*$ . Generally, introducing an appropriately chosen coarsening function  $w(\mathbf{x})$ , it can be evaluated as

$$\begin{aligned} \rho_w(\mathbf{x}_j^*, t) &= \int w(\mathbf{x}_j^* - \mathbf{x}) \rho_w(\mathbf{x}, t) d^3 x \\ &= \sum_{i=1}^{N_s} \xi_i m_i(t) w(\mathbf{x}_j^* - \mathbf{x}_i(t)). \end{aligned}$$

Here  $w$  satisfies  $\int w(\mathbf{x}) d^3 x = 1$ , and would be a piecewise linear, localized function with length-scale comparable to the grid width. If a super-droplet is simply shared by the 8 adjacent grid points at the corner of the cell, then  $w(\mathbf{x}) = 1/8\Delta V$  inside the cube with volume  $8\Delta V$ , and  $w(\mathbf{x}) = 0$  outside the cube.

SDM has been defined completely and the numerical simulation schemes have been also proposed. This is the main result of the present paper. In the next section, we show a preliminary result of SDM.

## V. DEMONSTRATION

A very preliminary result of a shallow maritime cumulus formation initiated by a warm bubble is presented in this section to demonstrate the practicality of SDM.

The simulation domain is 2-dimensional ( $x$ - $z$ ), 12.8 km in horizontal direction and 5.12 km in vertical direction. Initially, a humid but not saturated atmosphere is stratified, which is almost absolutely unstable under 2 km in altitude. There is a temperature inversion layer above 2 km. The equations below determines the initial base sounding of the atmosphere.

$$\begin{aligned} \mathbf{U}(\mathbf{x}, t = 0) &= 0, \\ T(x, z = 0, t = 0) &= 305.0 \text{ K}, \\ P(x, z = 0, t = 0) &= 101325 \text{ Pa}, \\ \frac{\partial T}{\partial z} &= \begin{cases} -9.5 \text{ K km}^{-1} & \text{if } z < 2.0 \text{ km}, \\ +3.0 \text{ K km}^{-1} & \text{if } z \geq 2.0 \text{ km}, \end{cases} \\ q_v(\mathbf{x}, t = 0) &= 0.022 \exp \left[ - \left\{ \frac{(z + 200.0 \text{ m})}{2000.0 \text{ m}} \right\}^2 \right]. \end{aligned}$$

The upper and lower boundary is fixed to their initial value and the horizontal boundary is periodic. A warm

bubble is inserted at the center of the horizontal axis according to the equation below.

$$\begin{aligned} \theta(\mathbf{x}, t = 0) &= \theta_b(\mathbf{x}, t = 0) + 1.0 \text{ K} \\ &\times \exp \left[ - \left\{ \frac{(z - 500.0 \text{ m})}{400.0 \text{ m}} \right\}^2 - \left\{ \frac{(x - 6.4 \text{ km})}{1200.0 \text{ m}} \right\}^2 \right], \end{aligned}$$

where  $\theta_b(\mathbf{x}, t = 0)$  is the base state of potential temperature.

We simulate the cloud dynamics according to the non-hydrostatic model introduced in Sec. II B with the numerical schemes proposed in Sec. IV B. The grid width is  $\Delta x = 3.125 \text{ m}$  and  $\Delta z = 4.0 \text{ m}$  with time step  $\Delta t = 0.0125 \text{ s}$ . We set the artificial viscosity  $\nu = \kappa = 1.56 \text{ m}^2 \text{ s}^{-1}$ .

Initially, NaCl CCNs are uniformly distributed in space with number density  $1.0 \times 10^7 \text{ m}^{-3}$ . The solute mass  $M_i(t = 0)$  has an exponential distribution given by the probability density

$$p(M_i) = \frac{1}{M_0} \exp \left( -\frac{M_i}{M_0} \right), \quad M_0 = 1.0 \times 10^{-16} \text{ g}.$$

Because it is unsaturated at the beginning, the growth equation (2) has a stable and steady solution, which is adopted as the initial value of the radius  $R_i(t = 0)$ . The coalescence efficiency used in Sec. IV A 6 is also adopted to this simulation.

For the numerical simulation of the microphysics processes, we also use the numerical scheme proposed in Sec. IV. Initially, the super-droplets are uniformly distributed in space with number density  $1.92 \text{ m}^{-3}$  with common multiplicity, i.e.,  $\xi_i(t = 0) = \text{INT}(1.0 \times 10^7 / 1.92) = 5208333$ . The grid for our Monte Carlo scheme of stochastic coalescence is same to that of non-hydrostatic model. The time steps are  $\Delta t_m = \Delta t_g = 1.0 \text{ s}$  and  $\Delta t_c = 10.0 \text{ s}$ .

Cloud started to form at about 8 min and began to rain at about 20 min. After raining for half an hour, the cloud remained for a while but finally disappeared at about 90 min. The amount of precipitation is about 1 mm in total. Figure 3 is a snapshot at the time 1608 s. We plot all the super-droplets with the color and the alpha transparency which are determined by their radius  $R_i$  and multiplicity  $\xi_i$ . The color map is indicated in the figure and the alpha value is determined by  $\alpha_i = 7.8 \times 10^{-5} (R_i / 10^{-3} \text{ m})^2 \xi_i$ , which is proportional to  $R_i^2 \xi_i$ . We can see that there is a turbulent like structures inside the cloud. Note that there are super-droplets also in the black region, but it is not depicted in this figure because the radius is very small, which represent CCNs.

In this section, we showed a very preliminary result of a shallow maritime cumulus formation initiated by a warm bubble, and demonstrated that SDM actually works as a cloud resolving model. Application to more realistic situations are our future works.

## VI. DISCUSSIONS

### A. extension of Super-Droplet Method

In Sec. IV, SDM was developed only for warm rain with only one soluble substance as the CCN. However, it is very conceivable that we can extend SDM to incorporate various properties of clouds, such as, several types of ice crystals, several sorts of soluble/insoluble CCNs, their chemical reactions, electrification, and the breakup of droplets. Here, we give a rough overview of how to achieve these extensions.

For this purpose, let us extend the type of attributes  $\mathbf{a}$ . To treat several kinds of soluble/insoluble chemicals for the CCNs, new attributes are necessary to represent the mass of each chemicals. To treat several types of ice crystals, one attribute may represent the state of the super-droplets. Additional attributes may represent the electric charge and the temperature of the droplet. If we do not give a terminal velocity, then the velocity of a droplet is also an independent attribute.

Let us denote the attributes of our new super-droplet as  $\mathbf{a}(t) = (a^{(1)}, a^{(2)}, \dots, a^{(d)})$ , where  $d$  is the number of independent attributes. Then, we have to give a time evolution law for each attributes, which determines the individual dynamics of super-droplets:

$$\frac{d\mathbf{a}_i}{dt} = \mathbf{f}(\mathbf{a}_i, \mathbf{A}(\mathbf{x}_i)), \quad i = 1, 2, \dots, N_s(t), \quad (26)$$

where  $\mathbf{A}(\mathbf{x}_i)$  represents the field variable which characterize the state of ambient atmosphere. Equation (26) may include the growth equation (2) and the time evolution of solute mass  $dM_i/dt = 0$ . For example, the chemical reactions and the electrification process may be also incorporated in (26).

The coalescence process must be specified for our new super-droplets. At first, we have to determine what kind of real-droplet  $\mathbf{a}'$  will be created after the coalescence of real-droplets  $\mathbf{a}_j$  and  $\mathbf{a}_k$ . This can be either deterministic or stochastic. Then, the coalescence of super-droplets will be determined similarly to (14)-(21). It is not the case in (17) and (21), but we may also change the position of super-droplets after the coalescence if necessary. Similar to (3), the coalescence probability for real-droplets must be given in the form

$$\begin{aligned} P_{jk} &= C(\mathbf{a}_j, \mathbf{a}_k) \frac{\Delta t_c}{\Delta V} |\mathbf{v}_j - \mathbf{v}_k| \\ &= \text{probability that real-droplet } j \text{ and } k \\ &\quad \text{inside the small region } \Delta V \text{ will coalesce} \\ &\quad \text{in the short time interval } (t, t + \Delta t_c), \end{aligned}$$

which in general is a function of the attributes  $\mathbf{a}_j$  and  $\mathbf{a}_k$ . Then the coalescence probability for super-droplets will be determined by (22).

The coalescence process is a short time and short range interaction between the droplets, but we may also consider other types of interactions if any.

Breakup of droplets can be also taken into account. This can be done if a governing law is given for the breakup process. However, note here that breakup results in the increase of super-droplets, and this is not preferable because the more the super-droplet is the more the computational cost will be. Breakup process may result in the explosion of the number of super-droplets  $N_s(t) \rightarrow \infty$ . In other words, SDM is formulated suitable for the simulation of such phenomena in which the coalescence process is predominant and the breakup process has a secondary importance. This is exactly the case for cloud formation process.

SDM can be regarded as a sort of Direct Simulation Monte Carlo (DSMC) method, which was initially proposed to simulate the Boltzmann equation for predicting rarefied gas flows (Bird 1994). Particularly, SDM has similarity to the Extended version of the No-Time-Counter (ENTC) method, which was developed by Schmidt and Rutland (2000) for the simulation of spray flows. Though the basic idea of using a computational particle with varying multiplicity is common in both SDM and ENTC, there is a difference in the procedure of the Monte Carlo scheme. SDM is using randomly generated, non-overlapping,  $[n_s/2]$  number of candidate pairs, and allows multiple coalescence for each pair. On the other hand, ENTC method chooses the candidate pairs randomly from the set of all the possible pairs. The number of candidate-pairs to be sampled varies proportionally to the maximum coalescence probability in the cell. Both SDM and ENTC method result in the computational cost  $O(N_s)$ . Probably, ENTC method is also applicable to cloud simulations and SDM is applicable to spray simulations, but further verifications are still necessary to compare their capability.

### B. computational cost and accuracy

Our estimation suggest that the computational cost of SDM becomes much lower than spectral (bin) method when the number of attributes  $d$  becomes large. We would like to show the basis of this assertion very briefly.

Let us estimate the computational cost and accuracy of spectral (bin) method. We have extended SDM in the previous section, and the corresponding, general form of SCE can be derived as follows.

$$\frac{\partial n(\mathbf{a}, \mathbf{x}, t)}{\partial t} + \nabla_x \cdot \{\mathbf{v}n\} + \nabla_a \cdot \{\mathbf{f}n\} = \left( \frac{\partial n}{\partial t} \right)_c, \quad (27)$$

where  $n(\mathbf{a}, \mathbf{x}, t)$  is the number density distribution and  $\mathbf{f}$  is defined in (26). The term  $(\partial n / \partial t)_c$  corresponds to the stochastic coalescence process and this will be  $d$ -multiple integral in general because we have to survey all over the  $d$ -dimensional attribute-space to evaluate the variation of droplet number density at  $\mathbf{a}$ . Obviously, this term is the most expensive for computation, so we neglect the advection terms in the l.h.s of (27) and focus our attention on the simplified equation  $\partial n / \partial t = (\partial n / \partial t)_c$ , which

corresponds to the ideal case that only the stochastic coalescence exists as the microphysics process.

We choose Integrated Squared Error (ISE),

$$C = \int d^d a \{n(\mathbf{a}) - n_b(\mathbf{a})\}^2, \quad (28)$$

to evaluate the accuracy of spectral (bin) method. Here,  $n_b(\mathbf{a})$  is the approximate solution generated by spectral (bin) method, and  $C$  evaluate the difference of  $n_b(\mathbf{a})$  from the exact solution  $n(\mathbf{a})$ . Let  $N_b$  be the number of bins for each attribute, i.e., the number of grid points for the discretization of  $n(\mathbf{a})$  per attribute. Then, if the accuracy of spectral bin method is  $k$ th order in attribute-space,  $C$  scales like  $C \sim N_b^{-2k}$ . Thus, we can estimate the amount of *operation count* and *memory* needed for the computation of spectral (bin) method as the following,

$$\begin{aligned} \text{operation} &\sim N_b^{2d} \sim \left(\frac{1}{\sqrt{C}}\right)^{2d/k}, \\ \text{memory} &\sim N_b^d \sim \left(\frac{1}{\sqrt{C}}\right)^{d/k}. \end{aligned} \quad (29)$$

Let us estimate the computational cost and accuracy of SDM. To compare the result with spectral (bin) method, we only consider the stochastic coalescence process, and let us estimate the number density distribution  $n(\mathbf{a})$  from the super-droplets  $\{(\xi_i, \mathbf{a}_i); i = 1, 2, \dots, N_s\}$  using the kernel density estimation method, which was originally developed to estimate the generating probability distribution from its random sample (Terrell and Scott 1992). The density estimator function  $\tilde{n}(\mathbf{a})$  with Gaussian kernel  $W_\sigma^{(d)}(\mathbf{a})$  is defined by

$$\begin{aligned} \tilde{n}(\mathbf{a}) &:= \sum_{i=1}^{N_s} \xi_i W_\sigma^{(d)}(\mathbf{a} - \mathbf{a}_i), \\ W_\sigma^{(d)}(\mathbf{a}) &:= \frac{1}{(\sqrt{2\pi}\sigma)^d} \exp\{-\mathbf{a}^2/2\sigma^2\}. \end{aligned} \quad (30)$$

The error function corresponding to ISE (28) is the Mean Integrated Squared Error (MISE) defined by

$$C(\sigma) = E \left[ \int d^d a \{n(\mathbf{a}) - \tilde{n}(\mathbf{a})\}^2 \right]. \quad (31)$$

Remember that each  $\{(\xi_i, \mathbf{a}_i)\}$  is a random realization and  $C(\sigma)$  is defined as an ensemble averaged value. Several calculations and assumptions are necessary to derive the results, but we can estimate the expectation value and variance of  $\tilde{n}(\mathbf{a})$  as

$$\begin{aligned} E[\tilde{n}(\mathbf{a})] - n(\mathbf{a}) &\simeq \frac{\sigma^2}{2} \left\{ \sum_j \frac{\partial^2 n(\mathbf{a})}{\partial a_j^2} \right\}, \\ V[\tilde{n}(\mathbf{a})] &\simeq \frac{N_r n(\mathbf{a})}{N_s (2\sqrt{\pi}\sigma)^d}. \end{aligned}$$

After some calculation, this result in

$$\sigma \sim N_s^{\frac{-1}{(d+4)}}, \quad C(\sigma) \sim N_s^{\frac{-4}{(d+4)}}.$$

Thus, the *operation count* and *memory* needed for SDM scales like

$$\begin{aligned} \text{operation} &\sim N_s \sim \left(\frac{1}{\sqrt{C(\sigma)}}\right)^{(d+4)/2}, \\ \text{memory} &\sim N_s \sim \left(\frac{1}{\sqrt{C(\sigma)}}\right)^{(d+4)/2}. \end{aligned} \quad (32)$$

We can compare the computational efficiency of SDM and spectral (bin) method by comparing the exponents in (29) and (32). The result suggest that the operation count of SDM becomes lower than spectral (bin) method when the condition

$$d > \frac{4k}{4-k} \quad \text{and} \quad k < 4,$$

is satisfied, and the memory of SDM becomes lower than spectral (bin) method when

$$d > \frac{4k}{2-k} \quad \text{and} \quad k < 2.$$

Thus, if we assume that the attribute-spatial accuracy of spectral (bin) method  $k = 1 \sim 2$ , SDM becomes more efficient in operation count when  $d > 2 \sim 4$ , and becomes efficient in memory when  $d > 4 \sim \infty$ . This result may be improved if we choose a different kernel function  $W(\mathbf{a})$  for the density estimator  $\tilde{n}(\mathbf{a})$ .

Though our discussions in this section are very brief and the assertions must be still verified, our estimation suggests that the computational cost of SDM becomes lower than spectral (bin) method when the number of attributes  $d$  becomes larger than some critical value, which may be  $2 \sim 4$ .

## VII. SUMMARY AND CONCLUDING REMARKS

In this paper, we introduced a simple SDM for warm rain and discussed the theoretical foundations and characteristics of SDM.

The principle model was introduced at the beginning, which is a very primitive microphysics-macrodynamics coupled cloud model. We saw how the traditional methods can be derived from the principle model and what are the problems involved in these methods. Then, we developed a simple SDM for warm rain, which can be regarded as a coarse-grained model of the principle model. Several numerical simulation schemes for SDM were also proposed. Especially, a novel Monte Carlo scheme for the stochastic coalescence process was developed and validated by comparing the numerical results with the solutions of SCE. We demonstrated the practicality of SDM

by presenting a very preliminary result of a shallow maritime cumulus formation initiated by a warm bubble. Brief discussions were carried out on the possibility to extend SDM to incorporate various properties of clouds, such as, several types of ice crystals, several sorts of soluble/insoluble CCNs, their chemical reactions, electrification, and the breakup of droplets. The assertions must be still verified, but our theoretical estimation suggested that SDM becomes computationally more efficient than spectral (bin) method when the number of attributes  $d$  becomes larger than some critical value, which may be  $2 \sim 4$ .

Though several extensions and validations are still necessary, we expect that SDM would be more feasible for the modeling of complicated cloud microphysics, and provide us a new approach to the cloud-related open problems, such as the cloud and aerosol interactions, the cloud-related radiative processes, and the mechanism of thunderstorms and lightning.

### Acknowledgments

The authors are grateful to A. Bott for offering his Fortran program, F. Araki for fruitful discussions, and T. Sato for his continued support. S.S. would like to thank T. Miyoshi, S. Hirose, H. Nakao, and R. Onishi for valuable comments and encouragement. This work is one of the results of the Earth Simulator project “Development of Multi-scale Coupled Simulation Algorithm.”

### APPENDIX: HOW TO MAKE A RANDOM PERMUTATION

Let  $a^{(n)} = (a_1^{(n)}, a_2^{(n)}, \dots, a_n^{(n)})$  be a permutation of  $I_n := (1, 2, \dots, n)$ . Let  $S_n := \{a^{(n)}\}$  be the set of all the permutation of  $I_n$ . Thus,  $S_n$  has  $n!$  number of elements. Let us define the *random permutation* of  $I_n$  by such a permutation  $a^{(n)}$  that all the  $a^{(n)} \in S_n$  occurs with the same probability, i.e.,  $P(a^{(n)}) = 1/n!$ ,  $\forall a^{(n)} \in S_n$ .

We have two propositions. 1)  $a^{(1)} = (1)$  is a random permutation of  $I_1$ . 2) We can make a random permutation of  $I_{n+1}$  from a random permutation of  $I_n$  by the following procedure: Let  $a^{(n)}$  be a random permutation of  $I_n$  and choose  $m$  from  $1, 2, \dots, n+1$  randomly. Let  $a^{(n+1)} = (a^{(n)}, n+1) = (a_1^{(n)}, \dots, a_n^{(n)}, n+1)$ . If  $m \neq n+1$ , exchange the value at  $m$  and  $n+1$ , i.e.,  $a_{n+1}^{(n+1)} = a_m^{(n)}, a_m^{(n+1)} = n+1$ . Then,  $a^{(n+1)}$  is a random permutation of  $I_{n+1}$ .

Proposition 1) is obvious and 2) is also easy to prove. For all  $a^{(n+1)} \in S_{n+1}$ , we can uniquely determine  $a^{(n)} \in S_n$  which have the possibility to become  $a^{(n+1)}$ . Indeed, such  $a^{(n)}$  is given by  $a^{(n)} = (a_1^{(n+1)}, a_2^{(n+1)}, \dots, a_{m-1}^{(n+1)}, a_{n+1}^{(n+1)}, a_{m+1}^{(n+1)}, \dots, a_n^{(n+1)})$ , here  $m$  satisfies  $a_m^{(n+1)} = n+1$ . If  $m = n+1$ ,  $a_i^{(n)} = a_i^{(n+1)}$ ,  $i = 1, \dots, n$ . Then, the probability that  $a^{(n+1)}$  occurs is evaluated by  $P(a^{(n+1)}) = P(a^{(n)}) \times 1/(n+1) = 1/(n+1)!$ .

Consequently, we can make a random permutation of  $I_n$  with  $O(n)$  operations.

---

[1] Beard, K. V., 1976: Terminal velocity and shape of cloud and precipitation drops aloft. *J. Atoms. Sci.*, **33**, 851–864.

[2] Berry, E. X., 1967: Cloud droplet growth by collection. *J. Atmos. Sci.*, **24**, 688–701.

[3] Bird, G. A., 1994: *Molecular gas dynamics and the direct simulation of gas flows*. Clarendon Press, Oxford, 458 pp.

[4] Bott, A., 1998: A flux method for the numerical solution of the stochastic collection equation. *J. Atmos. Sci.*, **55**, 2284–2293.

[5] — 2000: A flux method for the numerical solution of the stochastic collection equation: Extension to two-dimensional particle distributions. *J. Atmos. Sci.*, **57**, 284–294.

[6] Davis, M. H., 1972: *J. Atmos. Sci.*, **29**, 911–915.

[7] Ferrier, B. S., 1994: A double-moment multiple-phase four-class bulk ice scheme. part I: Description. *J. Atmos. Sci.*, **51**, 249–280.

[8] Gillespie, D. T., 1972: The stochastic coalescence model for cloud droplet growth. *J. Atmos. Sci.*, **29**, 1496–1510.

[9] — 1975: An exact method for numerically simulating the stochastic coalescence process in a cloud. *J. Atmos. Sci.*, **32**, 1977–1989.

[10] Golovin, A. M., 1963: The solution of the coagulation equation for cloud droplets in a rising air current. *Bull. Acad. Sci., USSR, Geophys. Ser.X*, **5**, 783–791.

[11] Hall, W. D., 1980: A detailed microphysical model within a two-dimensional dynamic framework - model description and preliminary-results. *J. Atoms. Sci.*, **37**, 2486–2507.

[12] Jacobson, M. Z., 2005: *Fundamentals of Atmospheric Modeling*. Cambridge Univ Press, New York, 2nd edition, 813 pp.

[13] Jonas, P. R., 1972: Collision efficiency of small drops. *Quart. J. Roy. Meteor. Soc.*, **98**, 681–683.

[14] Kessler, E., 1969: On the distribution and continuity of water substance in atmospheric circulations. *Meteor. Monogr.*, **10**, 1–84.

[15] Köhler, H., 1936: The nucleus in and the growth of hygroscopic droplets. *Trans. Faraday Soc.*, **32**, 1152–1161.

[16] Meyers, M. P., R. L. Walko, J. Y. Harrington, and W. R. Cotton, 1997: New RAMS cloud microphysics parameterization. part II: The two-moment scheme. *Atmos. Res.*, **45**, 3–39.

[17] Murakami, M., 1990: Numerical modeling of dynamical and microphysical evolution of an isolated convective cloud. *J. Meteor. Soc. Japan*, **68**, 107–128.

[18] Rogers, R. R. and M. K. Yan, 1989: *A Short Course in Cloud Physics*. Pergamon Press, Oxford, third edition, 293 pp.

[19] Schmidt, D. P. and C. J. Rutland, 2000: A new droplet collision algorithm. *J. Comput. Phys.*, **164**, 62–80.

[20] Seeßelberg, M., T. Trautmann, and M. Thorn, 1996: Stochastic simulations as a benchmark for mathematical methods solving the coalescence equation. *Atmos. Res.*, **40**, 33–48.

[21] Soong, S.-T., 1974: Numerical simulation of warm rain development in an axisymmetric cloud model. *J. Atmos. Sci.*, **31**, 1262–1285.

[22] Terrell, G. R. and D. W. Scott, 1992: Variable kernel density estimation. *Ann. Statist.*, **20**, 1236–1265.

[23] Ziegler, C. L., 1985: Retrieval of thermal and microphysical variables in observed convective storms. part i: Model development and preliminary testing. *J. Atmos. Sci.*, **42**, 1487–1509.

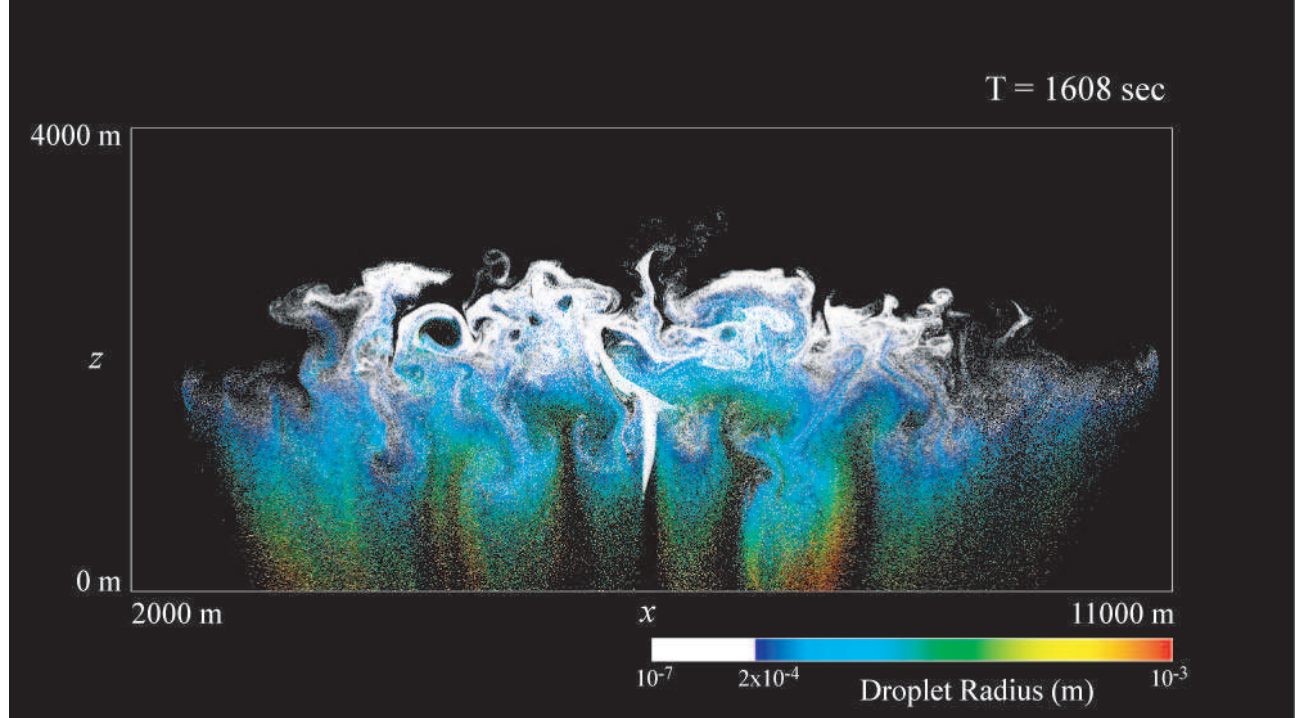


FIG. 3: Shallow maritime cumulus formation initiated by a warm bubble simulated by SDM. This is a snapshot at the time 1608 s. All the super-droplets are plotted with the color and the alpha transparency which are determined by their radius  $R_i$  and multiplicity  $\xi_i$ . The color map is indicated in the figure and the alpha value is determined by  $\alpha_i = 7.8 \times 10^{-5} (R_i/10^{-3} \text{ m})^2 \xi_i$ , which is proportional to  $R_i^2 \xi_i$ . We can see that there is a turbulent like structures inside the cloud.